ACS APPLIED MATERIALS & INTERFACES

Letter

www.acsami.org

Sintering of Ultrathin Gold Nanowires for Transparent Electronics

Johannes H. M. Maurer, Lola González-García,* Beate Reiser, Ioannis Kanelidis, and Tobias Kraus*

INM − Leibniz Institute for New Materials, Campus D2 2, 66123 Saarbrücken, Germany

Supporting Information

ABSTRACT: Ultrathin gold nanowires (AuNWs) with diameters below 2 nm and high aspect ratios are considered to be a promising base material for transparent electrodes. To achieve the conductivity expected for this system, oleylamine must be removed. Herein we present the first study on the conductivity, optical transmission, stability, and structure of AuNW networks before and after sintering with different techniques. Freshly prepared layers consisting of densely packed AuNW bundles were insulating and unstable, decomposing into gold spheres after a few days. Plasma treatments increased the conductivity and stability, coarsened the structure, and left the optical transmission virtually unchanged. Optimal conditions reduced sheet resistances to 50 Ω/sq.

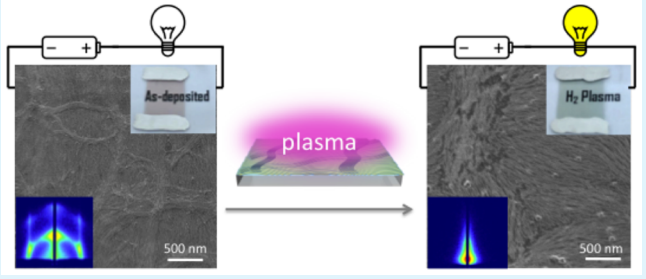

KEYWORDS: *metal nanostructures, capping ligands, ultrathin gold nanowires, AuNW layers, transparent electronics, soft sintering, GISAXS*

Transparent conductive materials (TCMs) are indispensable components of modern electronic devices such as thin-film displays, transparent solar cells, and touch screens. Most commonly encountered today is indium−tin oxide (ITO), which combines large optical transmittances of $T \approx 90\%$ with low sheet resistances in the range of $R_{sheet} \approx 10$ Ω/sq.[1] ITO and other transparent oxides have limitations when it comes to flexible and organic electronics, mainly because of their ceramic brittleness and high-temperature vacuum deposition. New classes of TCMs that could replace oxides in such applications include carbon nanotube networks,[2] graphene,[3] metal grids,[4] and metallic nanowire networks.[5] Metallic nanowire networks combine high conductivity with mechanical flexibility and can be deposited from liquid dispersions.[6] Silver nanowire (AgNW)[7] and copper nanowire[8] networks have been extensively studied and are now commercially competing with ITO.[9]

Since their first synthesis in 2007, ultrathin gold nanowires (AuNWs) with diameters below 2 nm[10−13] and high aspect ratios (>1000) have attracted great interest because of their mechanical flexibility[14,15] and high optical transparency.[16] Gold is more stable toward chemical degradation than silver and copper, while its conductivity achieves comparable values.[17] Sanchez-Iglesias et al.[16] and Chen et al.[15] prepared very thin conductive layers from AuNWs with high optical transparency ($T > 95\%$), proving the suitability of AuNWs as TCMs.

The conductivity of nanoparticle-based TCMs is often dominated by contact resistances between individual particles.[18,19] Large resistances are caused by capping ligands that surround the particles during synthesis and lend them colloidal stability. Isolating ligands act as tunnel barriers and hinder electron transport from particle to particle. For example, AuNWs are capped with oleylamine during synthesis, a molecule that is known to cause high junction resistances.[19] They are the main reason for AuNW films not to reach theoretically predicted conductivities.[15] Although the amount of oleylamine can be lowered by repeated washing of the AuNW suspension after synthesis, a certain amount of residual oleylamine is necessary to stabilize the thin structures in solution.[20]

Annealing is widely employed to lower the junction resistance in metal particle networks and to decrease the sheet resistance after layer formation. Thermal annealing,[21] plasma treatment,[22,23] and ligand exchange[19,24] have been reported to be effective treatments. However, not all of them are suitable for ultrathin AuNWs. Thermal annealing, which has successfully been applied to AgNWs,[21] would require temperatures far beyond the stability limit of AuNWs to remove the high-boiling oleylamine (bp = 350 °C). Because of their small diameters, AuNWs are extremely vulnerable to fragmentation by Rayleigh instability, which accelerates with increasing temperature.[25−28]

Reducing or oxidizing plasmas have been successfully used to remove organic compounds in nanoparticle systems.[22,23] A chemical alternative is ligand-exchange reaction in the dry film after deposition. Recently, Fafarman and co-workers[19,24] reported the exchange of oleylamine on spherical gold nanocrystals by ammonium thiocyanate (NH_4SCN). They observed a clear dielectric-to-metal transition after oleylamine was replaced by the short inorganic NH_4SCN. These methods have not been applied to ultrathin AuNWs so far.

Received: March 10, 2015
Accepted: April 2, 2015
Published: April 2, 2015

DOI: 10.1021/acsami.5b02088
ACS Appl. Mater. Interfaces 2015, 7, 7838−7842

In the following, we present a systematic study on the influence of reducing (5% hydrogen in argon, further referred to as hydrogen plasma) and oxidizing (pure oxygen) plasma treatment and ligand exchange on the structure, conductivity, and stability of ultrathin AuNW layers. We discuss the stability of the layers over time as a function of the annealing parameters.

A transmission electron microscopy (TEM) image of the as-synthesized ultrathin AuNWs is shown in Figure 1a. The wires had diameters of 1.6 nm, lengths of several micrometers. A homogeneous monolayer on the metal core should lead to a surface-to-surface spacing of 2−4 nm due to the interdigitation of the oleylamine molecules, as reported in the literature.[29] We deposited AuNW layers with a thickness of approximately 10 nm on glass by dip coating (see Methods in the Supporting Information, SI). A representative scanning electron microscopy (SEM) image of an as-deposited layer is shown in Figure 1b. Dense layers composed of AuNW "bundles" that were visible in SEM formed.[15] The photograph in Figure 1b shows the characteristic color of fresh layers that is due to the surface plasmon resonance of the AuNWs. Corresponding transmittance spectra can be found in the SI (Figure S1).

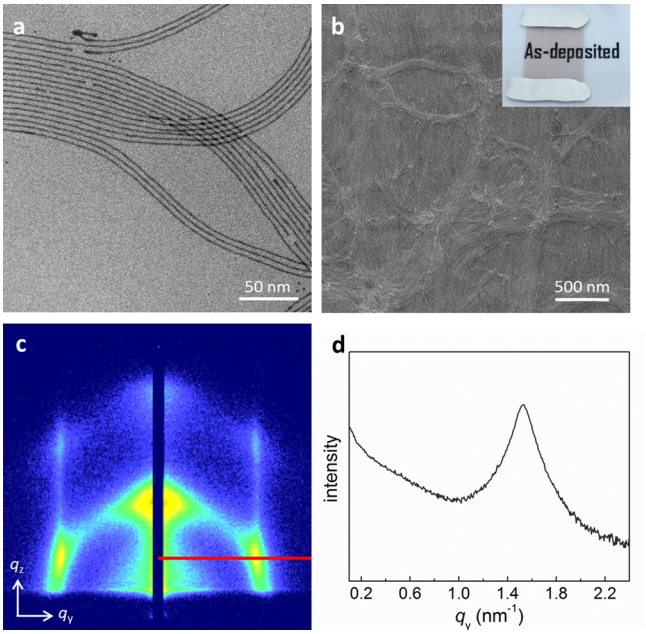

Figure 1. (a) TEM image of single AuNWs and (b) SEM image of a dense AuNW layer on glass as used in this work. The inset shows a photograph of the layer. (c) GISAXS pattern of an as-deposited AuNW layer. (d) Intensity distribution along the red bar in panel c.

Individual AuNWs are hardly visible in SEM images. To investigate the wire arrangement in the layer, grazing incidence small-angle X-ray scattering (GISAXS) measurements were performed. The pattern shown in Figure 1c indicates the presence of single wires. The peaks at $q_y = \pm 1.5$ nm^{-1} (see the horizontal intensity profile in Figure 1d) correspond to the average center-to-center distance of 4.2 nm.

Freshly deposited AuNW layers exhibited sheet resistances >40 MΩ, a value that is probably dominated by oleylamine tunnelling barriers between the metal nanostructures.

Figure 2 shows SEM images and sheet resistances after exposure to hydrogen plasma, oxygen plasma, and an ammonium thiocyanate solution. Plasma treatments readily decreased sheet resistances to the ohmic range, while immersion in an ammonium thiocyanate solution only decreased them to tens of megaohms, even after prolonged immersion.

Hydrogen plasma exposure for 1 min did not significantly change the appearance of the layer. Bundlelike structures remained visible in SEM, and the color appeared unchanged to the naked eye (Figure 2). GISAXS confirmed the existence of individual wires after annealing (see the inset in Figure 2), and optical UV−vis transmittance spectra remained largely unchanged (Figure S3 in the SI). Interestingly, 1 min of hydrogen plasma exposure decreased the sheet resistance to 200 kΩ/sq, probably by removing a fraction of oleylamine. Sustained exposure to hydrogen plasma caused a significant drop in the resistance to 50 Ω/sq. Thicker bundlelike structures became visible in SEM and indicated sintering of the nanowires. The scattering pattern characteristic for single wires had disappeared from GISAXS after 5 min, and only the Yoneda peak remained.[30] Exposure times above 15 min did not significantly improve the conductivity or alter the structure further. The sintering process is probably comparable with the

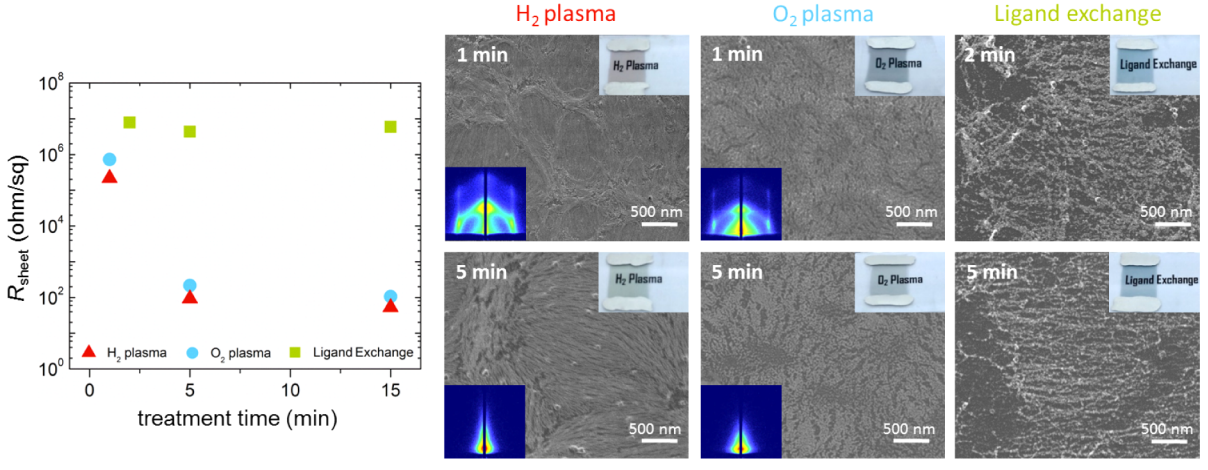

Figure 2. Sheet resistances (R_{sheet}) and layer structures according to SEM after exposure to hydrogen plasma, oxygen plasma, and an ammonium thiocyanate solution. Insets in the upper right corners show photographs of the different layers. GISAXS patterns for samples treated with plasma are shown as insets in the lower left corners. SEM images of layers treated for 15 min are shown in Figure S2 in the SI.

DOI: 10.1021/acsami.5b02088
ACS Appl. Mater. Interfaces 2015, 7, 7838−7842

"nanocrystal plasma polymerization" described by Cademartiri and co-workers that removes the capping ligands while retaining the overall nanocrystal arrangement.[31]

Oxygen plasma lowered the sheet resistances to values slightly above those found for hydrogen plasma. Sheet resistances remained in the megaohm range after 1 min and dropped to 200 Ω/sq after 5 min and to 100 Ω/sq after 15 min. In contrast to hydrogen, oxygen plasma drastically altered the morphology even after short treatments. Only weak X-ray scattering from single wires remained after 1 min (Figure 2), and their scattering was invisible after 5 min of annealing time. The changes in the morphology can be attributed to the fact that gold is not inert to the oxygen plasma. The slight oxidation of the surface to Au_2O_3 leads to large compressive stresses induced by the volume change.[32,33]

Ligand exchange only reduced the resistance to the megaohm range. Immersion of the layer in a 1% ammonium thiocyanate solution in acetone for 2 min, as used by Fafarman et al.,[19] led to obvious changes in the layer morphology. It appeared to mobilize the wires so that the films underwent morphological changes very different from those observed in gas-phase annealing. Longer immersion led to the formation of coarse agglomerates. An unknown fraction of AuNWs was lost to the solution despite the adhesion-increasing silanization of the substrates[19] (see the experimental details in the SI). Poor reproducibility due to wire loss and the large remaining sheet resistances make ligand exchange by NH_4SCN in acetone less suitable for ultrathin AuNWs and will therefore not be considered further here.

Morphology changes induced by annealing can improve or degrade the stability of the conductive layers. We measured the sheet resistances of freshly annealed layers as a function of the storage time under ambient conditions (Figure 3). Layers

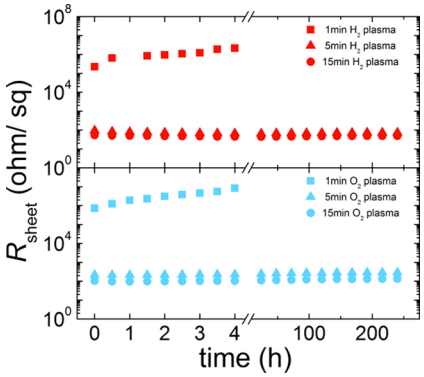

Figure 3. Sheet resistance (R_{sheet}) as a function of the storage time after treatment with hydrogen or oxygen plasma. Resistances of layers treated for 1 min exceeded the measurable range after 4 h.

treated with hydrogen and with oxygen plasma aged similarly: the sheet resistances of samples treated for 1 min significantly increased within the first hours, while samples treated for longer times retained their sheet resistances of around 50 Ω/sq (hydrogen) and 100 Ω/sq (oxygen) for at least 4 months.

The difference in the layer stability underpins our interpretation of the annealing mechanism. The Rayleigh instability rapidly degraded the original wires with 1.6 nm diameter in days even at room temperature.[27] Figure 4 shows electron micrographs of a sample recorded immediately after layer preparation (a) and after 1 week of storage at ambient conditions (d). Partial fragmentation into spheres is clearly

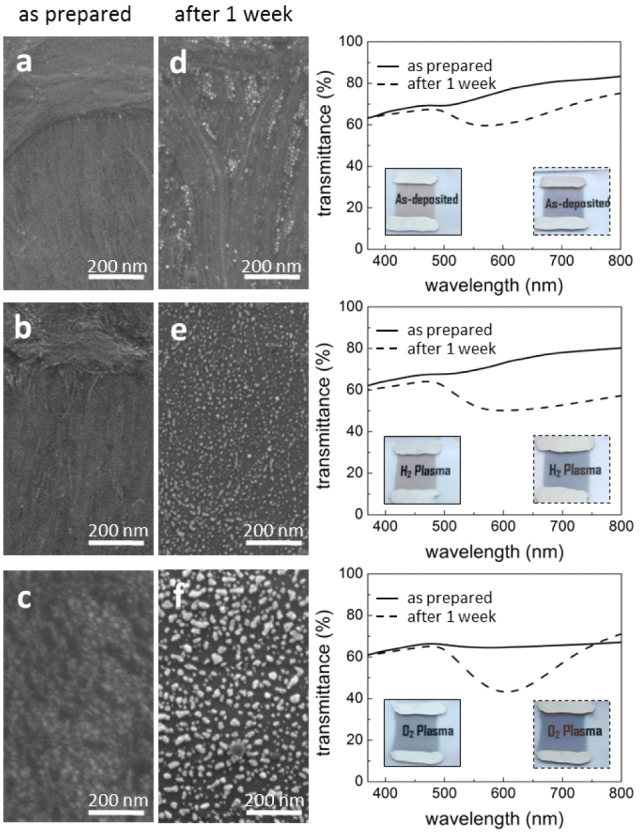

Figure 4. SEM images of AuNW layers recorded directly after (a) layer deposition, (b) 1 min of hydrogen plasma treatment and (c) 1 min of oxygen plasma treatment. (d–f) SEM images of the same samples after 1 week of storage under ambient conditions. The corresponding optical transmittance spectra are displayed on the right with optical photographs of the samples as insets.

visible and results in a color change from dark red to blue. Optical spectroscopy shows distinct surface plasmon resonance peaks that are indicative of spheres.

Short plasma treatments did not protect the layers but rather accelerated fragmentation: while untreated layers were stable for days, briefly annealed layers changed their color and sheet resistance already after hours (Figure 3). We believe that oleylamine protects the AuNW structure and that its partial removal during a short plasma treatment leads to acceleration of the fragmentation process. After 1 week, we found only spherical particles (Figure 4e,f) with sizes and particle-to-particle distances that were above those expected for the Rayleigh instability, probably indicating Ostwald ripening after fragmentation.[34] The sintered structures that formed after 5 min of plasma treatment did not exhibit the Rayleigh instability, and no structural change was observed with time.

In summary, this paper demonstrates that ultrathin AuNWs become suitable materials for transparent electronics after soft sintering. We dip-coated layers of transparent ultrathin AuNWs and found them to be insulating. The layer conductivity was readily increased after removal of oleylamine by annealing. Low-pressure hydrogen plasma treatment decreased the layers' sheet resistances while retaining optical transmission. Oxygen plasma treatment and solution-based ligand exchange were less effective.

Ultrathin AuNWs in freshly prepared layers consistently fragmented after a few days at ambient conditions. Partial

DOI: 10.1021/acsami.5b02088
ACS Appl. Mater. Interfaces 2015, 7, 7838–7842

removal of oleylamine in a short plasma treatment accelerated this degradation. Longer plasma treatments increased the layer stability to the point where no degradation was visible even after months. Optimal conditions led to sheet resistances of 50 Ω/sq, similar to a sputtered gold layer with a thickness of around 15 nm.

Annealing seemed to be most effective when it coarsened the layer morphology but retained some of its small-scale features. Electron microscopy and GISAXS indicated sintering of the AuNW into larger, filamentous structures. We believe that the plasma treatment converted nanowire bundles that were already present into stable wires. The sintered wires appear to be thin enough to avoid optical scattering and retain transparency.

Such "soft sintering" that retains some, but not all, features of a microstructure formed in solution is an interesting route to create materials with optimized properties from disperse nanoscale precursors.

■ ASSOCIATED CONTENT

Supporting Information

Experimental details, optical transmittance spectra of studied layers, SEM images and GISAXS measurements of samples treated for 15 min, and SEM images with different magnifications of samples treated for 5 min in hydrogen plasma. This material is available free of charge via the Internet at http://pubs.acs.org.

■ AUTHOR INFORMATION

Corresponding Authors

*E-mail: lola.gonzalez-garcia@inm-gmbh.de.
*E-mail: tobias.kraus@inm-gmbh.de.

Notes

The authors declare no competing financial interest.

■ ACKNOWLEDGMENTS

The authors thank Eduard Arzt for his continuing support of the project. Funding from the German Federal Ministry of Education and Research (BMBF) in the "NanoMatFutur" program is gratefully acknowledged.

■ REFERENCES

(1) De, S.; Higgins, T. M.; Lyons, P. E.; Doherty, E. M.; Nirmalraj, P. N.; Blau, W. J.; Boland, J. J.; Coleman, J. N. Silver Nanowire Networks as Flexible, Transparent, Conducting Films: Extremely High DC to Optical Conductivity Ratios. *ACS Nano* **2009**, *3*, 1767−1774.

(2) Artukovic, E.; Kaempgen, M.; Hecht, D. S.; Roth, S.; Gru, G. Transparent and Flexible Carbon Nanotube Transistors. *Nano Lett.* **2005**, *5*, 757−760.

(3) Wassei, J. K.; Kaner, R. B. Graphene, a Promising Transparent Conductor. *Mater. Today* **2010**, *13*, 52−59.

(4) Kang, M.-G.; Guo, L. Nanoimprinted Semitransparent Metal Electrodes and their Application in Organic Light-Emitting Diodes. *Adv. Mater.* **2007**, *19*, 1391−1396.

(5) Ye, S.; Rathmell, A. R.; Chen, Z.; Stewart, I. E.; Wiley, B. J. Metal Nanowire Networks: The Next Generation of Transparent Conductors. *Adv. Mater.* **2014**, *26*, 6670−6687.

(6) Lee, J.-Y.; Connor, S. T.; Cui, Y.; Peumans, P. Solution-processed Metal Nanowire Mesh Transparent Electrodes. *Nano Lett.* **2008**, *8*, 689−692.

(7) Langley, D.; Giusti, G.; Mayousse, C.; Celle, C.; Bellet, D.; Simonato, J.-P. Flexible Transparent Conductive Materials Based on Silver Nanowire Networks: a Review. *Nanotechnology* **2013**, *24*, 452001.

(8) Rathmell, A. R.; Bergin, S. M.; Hua, Y.-L.; Li, Z.-Y.; Wiley, B. J. The Growth Mechanism of Copper Nanowires and their Properties in Flexible, Transparent Conducting Films. *Adv. Mater.* **2010**, *22*, 3558−3563.

(9) Guo, C. F.; Ren, Z. Flexible Transparent Conductors Based on Metal Nanowire Networks. *Mater. Today* **2014**, *00*, 1−12.

(10) Halder, A.; Ravishankar, N. Ultrafine Single-Crystalline Gold Nanowire Arrays by Oriented Attachment. *Adv. Mater.* **2007**, *19*, 1854−1858.

(11) Wang, C.; Hu, Y.; Lieber, C. M.; Sun, S. Ultrathin Au Nanowires and their Transport Properties. *J. Am. Chem. Soc.* **2008**, *130*, 8902−8903.

(12) Feng, H.; Yang, Y.; You, Y.; Li, G.; Guo, J.; Yu, T.; Shen, Z.; Wu, T.; Xing, B. Simple and Rapid Synthesis of Ultrathin Gold Nanowires, their Self-assembly and Application in Surface-enhanced Raman Scattering. *Chem. Commun.* **2009**, 1984−1986.

(13) Cademartiri, L.; Ozin, G. A. Ultrathin Nanowires—A Materials Chemistry Perspective. *Adv. Mater.* **2009**, *21*, 1013−1020.

(14) Gong, S.; Schwalb, W.; Wang, Y.; Chen, Y.; Tang, Y.; Si, J.; Shirinzadeh, B.; Cheng, W. A Wearable and Highly Sensitive Pressure Sensor with Ultrathin Gold Nanowires. *Nat. Commun.* **2014**, *5*, 1−8.

(15) Chen, Y.; Ouyang, Z.; Gu, M.; Cheng, W. Mechanically Strong, Optically Transparent, Giant Metal Superlattice Nanomembranes from Ultrathin Gold Nanowires. *Adv. Mater.* **2013**, *25*, 80−85.

(16) Sánchez-Iglesias, A.; Rivas-Murias, B.; Grzelczak, M.; Pérez-Juste, J.; Liz-Marzán, L. M.; Rivadulla, F.; Correa-Duarte, M. A. Highly Transparent and Conductive Films of Densely Aligned Ultrathin Au Nanowire Monolayers. *Nano Lett.* **2012**, *12*, 6066−6070.

(17) Lyons, P. E.; De, S.; Elias, J.; Schamel, M.; Philippe, L.; Bellew, A. T.; Boland, J. J.; Coleman, J. N. High-Performance Transparent Conductors from Networks of Gold Nanowires. *J. Phys. Chem. Lett.* **2011**, *2*, 3058−3062.

(18) Hecht, D. S.; Hu, L.; Irvin, G. Emerging Transparent Electrodes Based on Thin Films of Carbon Nanotubes, Graphene, and Metallic Nanostructures. *Adv. Mater.* **2011**, *23*, 1482−1513.

(19) Fafarman, A. T.; Hong, S.-H.; Caglayan, H.; Ye, X.; Diroll, B. T.; Paik, T.; Engheta, N.; Murray, C. B.; Kagan, C. R. Chemically Tailored Dielectric-to-metal Transition for the Design of Metamaterials from Nanoimprinted Colloidal Nanocrystals. *Nano Lett.* **2013**, *13*, 350−357.

(20) Mourdikoudis, S.; Liz-Marzán, L. M. Oleylamine in Nanoparticle Synthesis. *Chem. Mater.* **2013**, *25*, 1465−1476.

(21) Langley, D. P.; Lagrange, M.; Giusti, G.; Jiménez, C.; Bréchet, Y.; Nguyen, N. D.; Bellet, D. Metallic Nanowire Networks: Effects of Thermal Annealing on Electrical Resistance. *Nanoscale* **2014**, *6*, 13535−13543.

(22) Jiang, H.; Vinod, T. P.; Jelinek, R. Spontaneous Assembly of Extremely Long, Horizontally-aligned, Conductive Gold Microwires in a Langmuir Monolayer Template. *Adv. Mater. Interfaces* **2014**, 1400187.

(23) Gehl, B.; Frömsdorf, A.; Aleksandrovic, V.; Schmidt, T.; Pretorius, A.; Flege, J.-I.; Bernstorff, S.; Rosenauer, A.; Falta, J.; Weller, H.; Bäumer, M. Structural and Chemical Effects of Plasma Treatment on Close-packed Colloidal Nanoparticle Layers. *Adv. Funct. Mater.* **2008**, *18*, 2398−2410.

(24) Fafarman, A. T.; Koh, W.-k.; Diroll, B. T.; Kim, D. K.; Ko, D.-K.; Oh, S. J.; Ye, X.; Doan-Nguyen, V.; Crump, M. R.; Reifsnyder, D. C.; Murray, C. B.; Kagan, C. R. Thiocyanate-Capped Nanocrystal Colloids: Vibrational Reporter of Surface Chemistry and Solution-based Route to Enhanced Coupling in Nanocrystal Solids. *J. Am. Chem. Soc.* **2011**, *133*, 15753−15761.

(25) Rayleigh, L. On the Stability of Jets. *Proc. London Math. Soc.* **1878**, *10*, 4−12.

(26) Toimil-Molares, M. E.; Balogh, A. G.; Cornelius, T. W.; Neumann, R.; Trautmann, C. Fragmentation of Nanowires Driven by Rayleigh Instability. *Appl. Phys. Lett.* **2004**, *85*, 5337−5339.

(27) Xu, J.; Zhu, Y.; Zhu, J.; Jiang, W. Ultralong Gold Nanoparticle/Block Copolymer Hybrid Cylindrical Micelles: a Strategy Combining Surface Templated Self-assembly and Rayleigh Instability. *Nanoscale* **2013**, *5*, 6344−6349.

DOI: 10.1021/acsami.5b02088
ACS Appl. Mater. Interfaces 2015, 7, 7838−7842

(28) Karim, S.; Toimil-Molares, M. E.; Balogh, A. G.; Ensinger, W.; Cornelius, T. W.; Khan, E. U.; Neumann, R. Morphological Evolution of Au Nanowires Controlled by Rayleigh Instability. *Nanotechnology* **2006**, *17*, 5954−5959.
(29) Loubat, A.; Impéror-Clerc, M.; Pansu, B.; Meneau, F.; Raquet, B.; Viau, G.; Lacroix, L.-M. Growth and self-assembly of ultrathin Au nanowires into expanded hexagonal superlattice studied by in situ SAXS. *Langmuir* **2014**, *30*, 4005−4012.
(30) Müller-Buschbaum, P. In *Applications of Synchrotron Light to Scattering and Diffraction in Materials and Life Sciences*; Gomez, M., Nogales, A., Garcia-Gutierrez, M. C., Ezquerra, T., Eds.; Lecture Notes in Physics; Springer: Berlin, 2009; Vol. *776*, pp 61−89.
(31) Cademartiri, L.; Ghadimi, A.; Ozin, G. A. Nanocrystal Plasma Polymerization: From Colloidal Nanocrystals to Inorganic Architectures. *Acc. Chem. Res.* **2008**, *41*, 1820−1830.
(32) Koslowski, B.; Boyen, H.; Wilderotter, C. Oxidation of preferentially (1 1 1)-oriented Au Films in an Oxygen Plasma Investigated by Scanning Tunneling Microscopy and Photoelectron Spectroscopy. *Surf. Sci.* **2001**, *475*, 1−10.
(33) Fuchs, P. Low-pressure Plasma Cleaning of Au and PtIr Noble Metal Surfaces. *Appl. Surf. Sci.* **2009**, *256*, 1382−1390.
(34) Gentry, S. T.; Kendra, S. F.; Bezpalko, M. W. Ostwald Ripening in Metallic Nanoparticles: Stochastic Kinetics. *J. Phys. Chem. C* **2011**, *115*, 12736−12741.

DOI: 10.1021/acsami.5b02088
ACS Appl. Mater. Interfaces 2015, 7, 7838−7842